



## STUDY OF TITANIUM ALUMINIUM NITRIDE DEPOSITED ON SILICON WAFER USING RF MAGNETRON SPUTTERING

Suman Choudhury\*, Suraj Kumar\*\* &  
Sanjay Kumar Sinha\*\*\*

Department of Applied Physics, Birla Institute of Technology Mesra,  
Ranchi, Jharkhand

**Cite This Article:** Suman Choudhury, Suraj Kumar & Sanjay Kumar Sinha, "Study of Titanium Aluminium Nitride Deposited on Silicon Wafer Using RF Magnetron Sputtering", International Journal of Multidisciplinary Research and Modern Education, Volume 4, Issue 1, Page Number 152-157, 2018.

**Copy Right:** © IJMRME, R&D Modern Research Publication, 2018 (All Rights Reserved). This is an Open Access Article distributed under the Creative Commons Attribution License, which permits unrestricted use, distribution, and reproduction in any medium provided the original work is properly cited.

### **Abstract:**

A thin layer of Titanium Aluminium Nitride was deposited on Silicon wafer by using reactive RF magnetron sputtering at a frequency of 13.56 MHz. The crystallite size and surface morphology of treated and untreated coatings was studied using Scanning Electron Microscope analysis and X-Ray diffraction. The corrosion current, corrosion rate and electrochemical behaviour was also determined using Electrochemical Analyzer test.

### **1. Introduction:**

The demand for deposition of coating materials with magnificent physical properties is always critical. The focus on developing thin film materials which are suitable for high temperature applications, high corrosive and erosive environments applications is highly increasing. So, withstanding the above mention conditions were necessary for various industrial applications. This research work studies efficient methods to create new coating materials which can be used for various types of applications. One of the most effective ways to create thin film materials of desired composition is sputtering process. Titanium Nitrides (TiN) coatings are one of the most commonly used thin films [1, 2]. TiAlN films exhibit better performance than TiN [3] because of the formation of an  $Al_2O_3/TiO_2$  oxide scale when in contact with air at higher temperature [4]. TiAlN films have been obtained by several deposition techniques, such as chemical vapor deposition, ion plating and physical vapor deposition (PVD) [5]. In this present work, hard TiAlN coatings were deposited using reactive RF magnetron sputtering of TiAl target in Ar + N<sub>2</sub> plasma atmosphere onto silicon substrates. As similar to this principle, generated plasma is used to ionize gas atoms which in turn strike the target surface. The impact emits atoms from the target material that will be transferred to the substrate surface and deposit coatings of required composition. The sputtering yield 'S' (number of atoms ejected from the target surface per incident ion) depends on the target material composition, binding energy, characteristics of the incident ion and the experimental geometry. It also depends on the voltage and current (sputter power) at which sputtering takes place. Sputtering deposition is more superior than other Physical Vapor Deposition processes as it provides better adhesion to deposited materials, have simpler mechanism, film-uniformity [6] & certain other novel properties in comparison to other methods. TiAlN coated Si has wide range of application in the field of bio-implants, corrosion resistant parts & electronics industry.

### **2. Experimental:**

#### **A. Materials:**

The formation of TiAlN from Titanium aluminium (TiAl) is done by adding a reactive gas in this case N<sub>2</sub> is supplied inside the vacuum chamber which reacts with the TiAl target alloy and forms TiAlN which is deposited on the substrate. Substrate used in this work is silicon (Si) wafer which is a semiconductor substrate material. The substrates which are used for coating deposition needs to be perfectly placed to achieve better deposition rate. Silicon have an indirect band gap of 1.12 eV and have a diamond like Face Centred Cubic (FCC) structure.

#### **B. RF Magnetron Sputtering System:**

The coating chamber of our RF Magnetron Sputtering system is fabricated out of 12 mm thick sheet of polished non-magnetic stainless steel of AISI 304L. The chamber is provided with a door at the front and it contains one view port of 5inch diameter and two dummy ports of 2inch diameter for further investigation, online diagnostic and plasma analysis. The substrate shutter is also provided to prevent the sputtering of the substrate when we are sputter cleaning the targets. The chamber consists of the provision for the insertion of the electrode from the top. The chamber contains a provision for inletting the gases from the mass flow meters. Target to substrate distance is 5cm.

The pumping system consists of a turbo molecular pump (TMP) backed by a rotary pump. There is a throttle valve with adjustable opening between the deposition chamber and the vacuum system to maintain a dynamic vacuum in the chamber by balancing the evacuation rate and rate of Ar gas injection in the chamber.

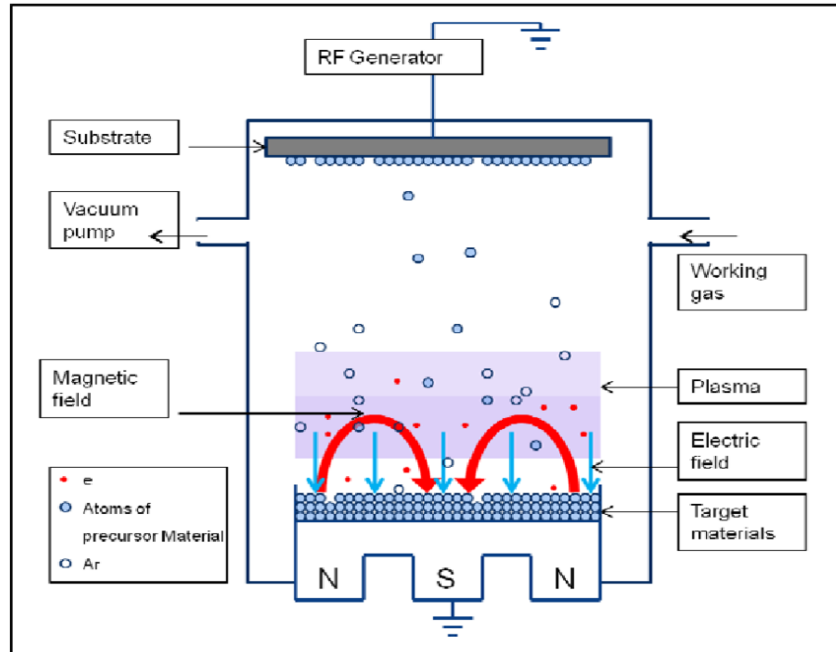


Figure 1: Schematic representation of magnetron sputtering [7]

### C. X-Ray Diffraction (XRD):

The X-ray diffraction profiles of our sample was recorded with a Rigaku Smart Lab diffractometer using Photon Max high-flux 9 kW rotating anode X-ray source coupled with a HyPix-3000 high-energy-resolution 2D multidimensional semiconductor detector. The diffractometer uses Cu-K $\alpha$  radiation (wavelength of about 1.54Å).

### D. Electrochemical Analyzer (ECA):

The basic principle of corrosion is the formation of electrolyte due to thin film of moisture on a metal surface for atmospheric corrosion. The corrosion resistance of material is an important factor in determining its biocompatibility. Every implant material corrodes inside the human body. Different materials have different intrinsic aptitudes to corrode. The more noble the material, the lesser is its aptitude to corrode. The structure, composition and thickness of the passive layer are highly dependent on the material itself and its environment. Materials contain various elements, such as lattice defects, impurities and contaminants, which may affect the corrosion reaction. The different heat treatments and working processes change the grain size and energy state of the material and cause surface heterogeneity. All these factors may affect the passivation layer. Corrosion resistance of our samples were studied using Electrochemical Analyzer (ECA), model 660 Series, CHI Instruments, made in USA, located at BIT Mesra, Ranchi. For corrosion analysis, samples were immersed in Ringer solution (2.1 gm NaCl in 50 ml of distilled water; 3.5 wt% NaCl). Additional electrodes, counter electrode & saturated calomel electrodes are immersed in the solution, and all the electrodes are connected to a device called a potentiostat.

### E. Scanning Electron Microscope (SEM):

SEM is perhaps the most widely employed thin-film and coating characterization instrument. Electrons thermionically emitted from a tungsten lamp, cathode filament are drawn to an anode, focused by two successive condenser lenses into a beam with a very fine spot size ( $\approx 50 \text{ \AA}$ ) [8]. Surface topography and overview pictures of the coated substrate collected in the scanning electron microscope JEOL JSM-6390LV model. The tungsten filament of SEM utilizes a tilting and rotating mechanical stage. It incorporates low vacuum back-scattered electron imaging for acquisition of high-resolution images of non-conductive, unprocessed samples.

## 3. Results and Discussions:

### X-Ray Diffraction Analysis:

XRD provided information regarding crystal structure, since periodicity and symmetry are components of ordered crystal structures. Distortions or alterations to the periodic structure can also be observed through distortions in the x-ray diffractogram, this provides information regarding grain size, epitaxy and texture. We have compared the pattern through PCPDFWIN database.

From figure 2 we can find the average size associated with each different peak and also determine the crystal structure. The structure of deposited TiAlN is Face Centered Cubic (FCC) Structure. The crystallite size of the corresponding XRD peaks was calculated using Scherrer Equation [9].

- ✓ For the first peak (hkl) value of (006) at  $12.83^\circ$ , the crystallite size is 136.72 nm and the lattice strain is 0.0024.

- ✓ For the second peak (hkl) value of (111) at 12.59°, the crystallite size is 157.5 nm and the lattice strain is 0.0021.
- ✓ For the third peak (hkl) value of (1012) at 29.41°, the crystallite size is 126.21 nm and the lattice strain is 0.0011.
- ✓ For the fourth peak (hkl) value of (209) at 41.69°, the crystallite size is 47.51 nm and the lattice strain is 0.0021.

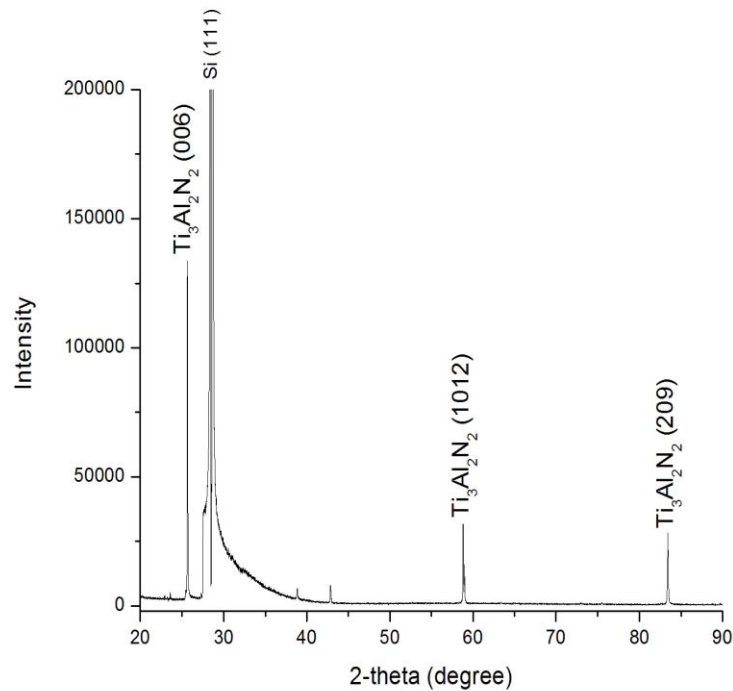


Figure 2: XRD plot for the TiAlN deposited on Silicon wafer

#### Electrochemical Analysis:

To determine the values of corrosion potential ( $E_C$ ) & corrosion current density ( $I_C$ ), extrapolated linear sections from anodic and cathodic curves are used. The corrosion rate per unit area of a material is expressed as a current density since the weight loss of a metal from a given area is proportional to the current density. The temperature of the solution during the measurement was kept constant at  $37.6 \pm 1^\circ\text{C}$ . The corrosion current ( $I_C$ ) and corrosion rate ( $C_R$ ) was determined using the software provided with the system.

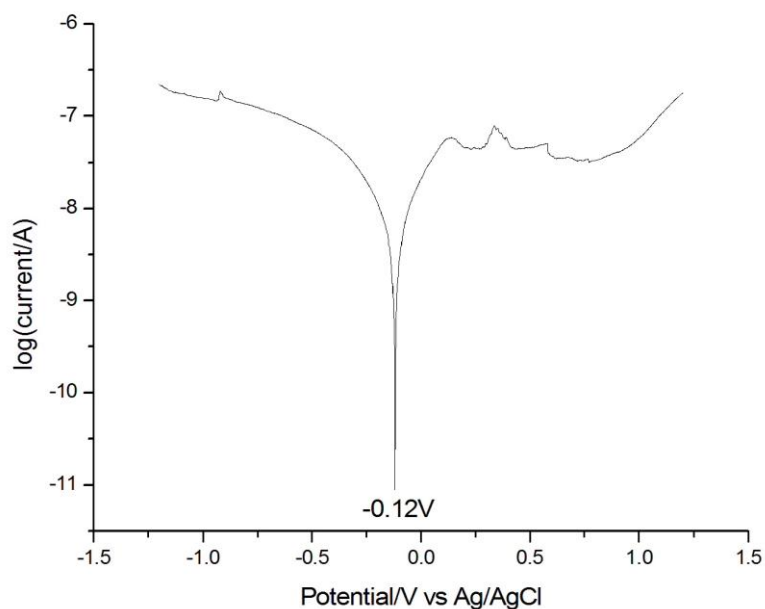


Figure 3: Tafel plot for coated Silicon wafer

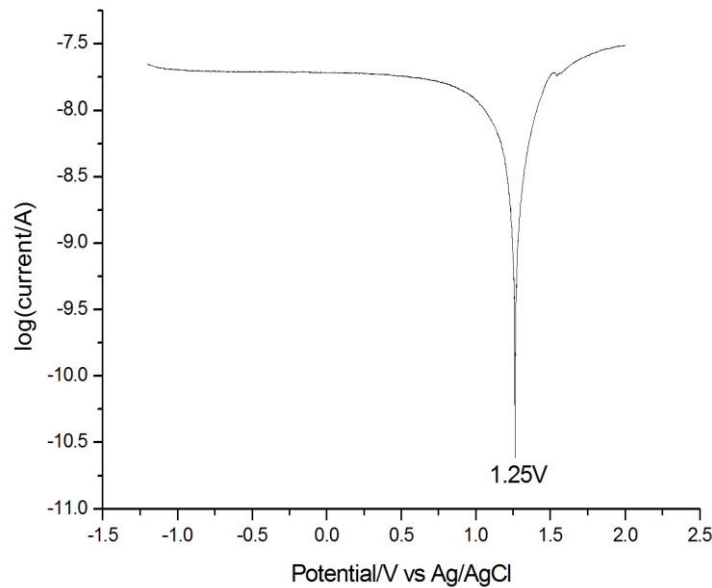


Figure 4: Tafel plot for uncoated Silicon wafer

The Tafel plot determines some specific parameters for the coatings such as the corrosion current and the corrosion rate. From Tafel plots figure 3 & 4, the corrosion rate of coated and uncoated Silicon wafers was found to be  $6.207 \times 10^{-3}$  mil/year and  $4.930 \times 10^{-3}$  mil/year respectively.

Substrates	Cathodic Tafel Slope	Anodic Tafel Slope	Corrosion Current ( $I_C$ ) Amperes	Corrosion Rate ( $C_R$ ) (mil/year)	Corrosion Rate ( $C_R$ ) (Angs/min)
Coated Si	4.62	5.123	$6.174 \times 10^{-9}$	$6.207 \times 10^{-3}$	$3.0 \times 10^{-3}$
Uncoated Si	3.373	5.249	$3.122 \times 10^{-9}$	$4.930 \times 10^{-3}$	$2.38 \times 10^{-3}$

Table 1: Shows the specific corrosion characteristics of the substrates after deposition

From table 1, the corrosion rate of coated Si is lower than that of uncoated Si. The Electro Chemical Analysis was done to both the coated sample as well as uncoated Si wafer. The Tafel Plots were obtained for both the cases.  $I_C$  was determined for both samples by these plots. It was found that the  $I_C$  for coated sample was less than that of uncoated sample. Also, the  $E_C$  of the uncoated sample is more than that of the coated sample. Hence, from these results we can conclude that the corrosion resistance of Si wafer is increased by coating it with a layer of TiAlN.

**Scanning Electron Microscope Analysis:**

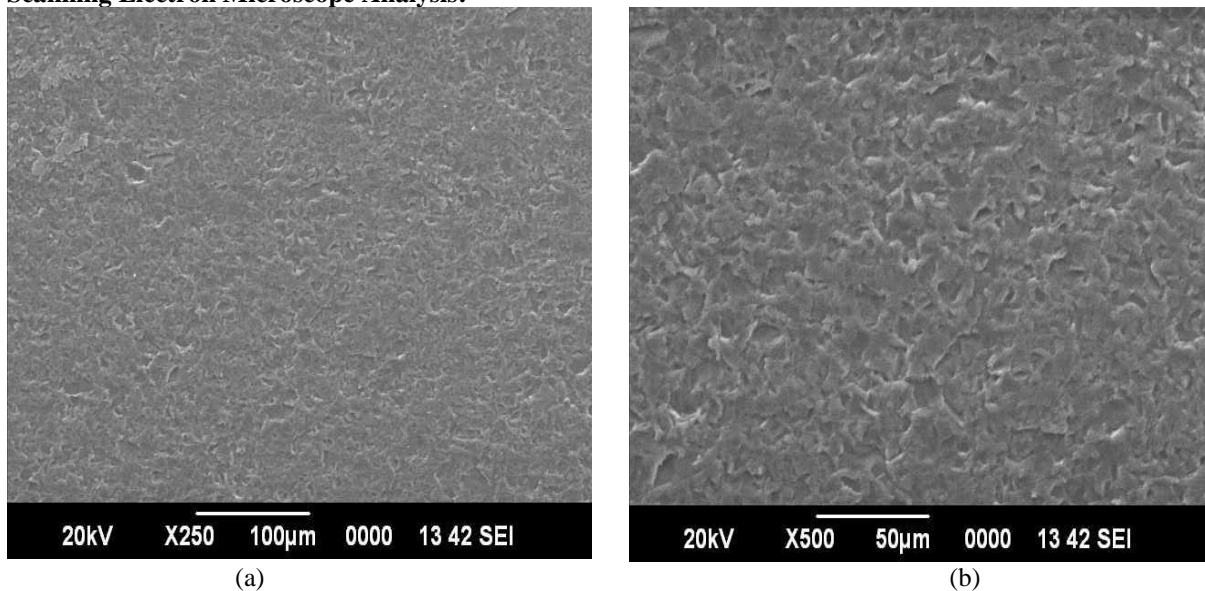
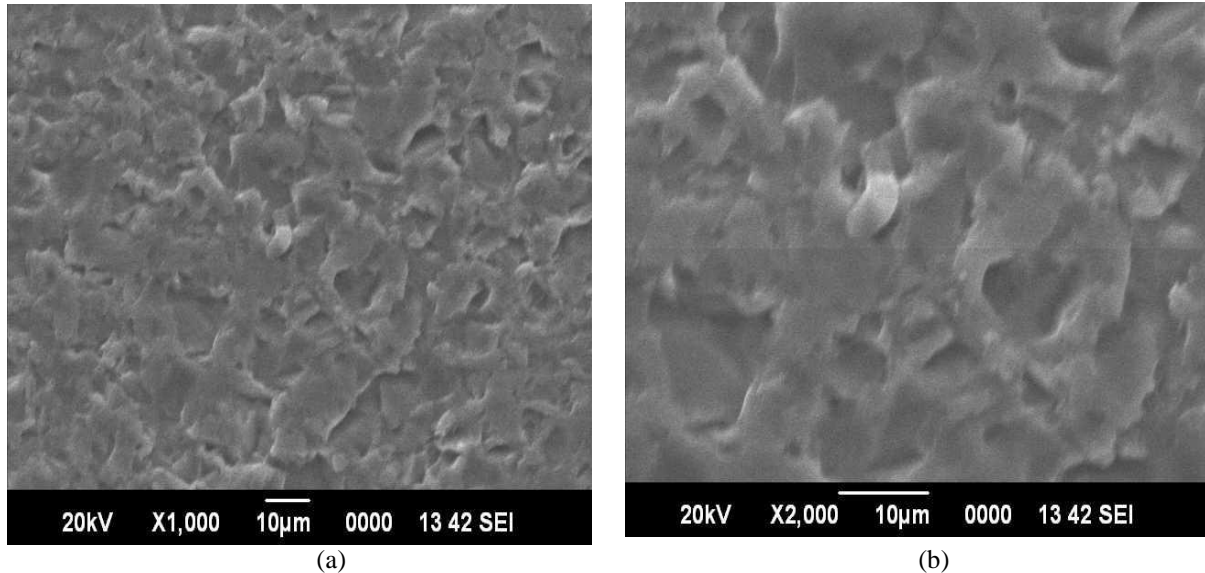


Figure 5: SEM images from investigation of coated Si surface at a magnification of (a) 250 & (b) 500



(a) (b)  
(b) Figure 6: SEM images from investigation of coated Si surface at a magnification of (a) 1000 & (b) 2000

The microstructure of TiAlN coating was studied using SEM. Fig 6(a) & 6(b) displays the top view of the SEM micrograph of the deposited TiAlN film. Geometry and texture of any coated surface can be evaluated by analysis of surface roughness. [10] The coating has a columnar structure and there thickness was estimated to be approximately 1.2  $\mu\text{m}$ . The coating is dense, uniform, homogeneous & compact. Sputtered coatings generally have a columnar structure and a smooth coating surface without the presence of macroparticles specially conventional sputtered (Ti,Al)N coatings.[11]. At the resolution of 2000X the image of a single grain was obtained. The crystalline size of these grains was determined by X-Ray diffraction analysis. The thickness of the deposition can be varied by controlling the flow of nitrogen supply. Increase in nitrogen flow rate decreases the thickness of the coating & vice versa. This happens because the density of the gas molecules increases with rising nitrogen flow rate, which leads to more collisions & reduced thickness [12].

#### 4. Conclusion:

TiAlN coatings were prepared & deposited onto a Si wafer substrate and the analysis of prepared sample was done by X-Ray Diffraction, Scanning Electron Microscope & Electrochemical Analyzer. We can finally conclude that RF Magnetron Sputtering deposition of TiAlN can be used to improve and incorporate some novel properties into the material. These improved materials have wide range of application in various fields such as bio implants, aerospace materials, corrosion resistant parts, electronics industries etc. The sputter deposition process is highly advantageous when it is used to its full potential. With this in mind and the experience gained during this research studies, the future work is planned to conduct with respect to manufacturing of alloy compounds. The sputtering equipment is running well and available for future research work of sputter coating of different materials, cryogenic treatment of Austenite Stainless steel or TiAlN coating on Perovskite.

#### 5. Acknowledgement:

This work was carried out with support of Mr Raj Kishore Pramanik who was responsible for the operation of RF Magnetron Sputtering deposition system stationed in the Plasma Laboratory, and the Central Instrumentation Facility (CIF) of BIT Mesra, Ranchi, India.

#### 6. References:

1. Su, G., & Liu, Z. (2012). Wear characteristics of nano TiAlN-coated carbide tools in ultra-high speed machining of AerMet100. *Wear*, 289, 124-131
2. Gnoth, C., Kunze, C., Hans, M., Emmerlich, J., Schneider, J. M., & Grundmeier, G. (2013). Surface chemistry of TiAlN and TiAlNO coatings deposited by means of high power pulsed magnetron sputtering. *Journal of Physics D: Applied Physics*, 46(8), 084003
3. Du, H., Xiong, J., Zhao, H., Wu, Y., Wan, W., & Wang, L. (2014). Structure and properties of TiAlLaN films deposited at various bias voltages. *Applied Surface Science*, 292, 688-694
4. Zhou, W., Liang, J., Zhang, F., Mu, J., & Zhao, H. (2014). A comparative research on TiAlN coatings reactively sputtered from powder and from smelting TiAl targets at various nitrogen flow rates. *Applied Surface Science*, 313, 10-18
5. Kim, G., Lee, S., & Hahn, J. (2005). Properties of TiAlN coatings synthesized by closed-field unbalanced magnetron sputtering. *Surface and Coatings Technology*, 193(1-3), 213-218

6. Suman Choudhury & Sanjay Kumar Sinha, "A Comparative Study of Mo Films Deposited on AISI 310 and Al<sub>2</sub>O<sub>3</sub> Surface Using Anodic Vacuum Arc", International Journal of Multidisciplinary Research and Modern Education, Volume 4, Issue 1, Page Number 146-151, 2018
7. Bosco, R., Van Den Beucken, J., Leeuwenburgh, S., & Jansen, J. (2012). Surface engineering for bone implants: a trend from passive to active surfaces. *Coatings*, 2(3), 95-119
8. Khairnar, A. G. (2015). Deposition and characterization of high k dielectric thin films for mos capacitors
9. Speakman, S. A. (2014). Estimating crystallite size using XRD. MIT Center for Materials Science and Engineering
10. Benardos, P. G., & Vosniakos, G. C. (2003). Predicting surface roughness in machining: a review. *International journal of machine tools and manufacture*, 43(8), 833-844
11. Ait-Djafer, A. Z., Saoula, N., Aknouche, H., Guedouar, B., & Madaoui, N. (2015). Deposition and characterization of titanium aluminum nitride coatings prepared by RF magnetron sputtering. *Applied Surface Science*, 350, 6-9
12. Obrosof, A., Gulyaev, R., Ratzke, M., Volinsky, A. A., Bolz, S., Naveed, M., & Weiß, S. (2017). XPS and AFM investigations of Ti-Al-N coatings fabricated using DC magnetron sputtering at various nitrogen flow rates and deposition temperatures. *Metals*, 7(2), 52